



Promoting the Insertion of Molecular Hydrogen in Tetrahydrofuran Hydrate With the Help of Acidic Additives

The Thuong Nguyen¹, Claire Pétuya^{1,2}, David Talaga¹ and Arnaud Desmedt^{1*}

¹ Groupe Spectroscopie Moléculaire, ISM, UMR5255 CNRS—University, Bordeaux, France, ² Jet Propulsion Laboratory, California Institute of Technology, Pasadena, CA, United States

Among hydrogen storage materials, hydrogen hydrates have received a particular attention over the last decades. The pure hydrogen hydrate is generated only at extremely high-pressure (few thousands of bars) and the formation conditions are known to be softened by co-including guest molecules such as tetrahydrofuran (THF). Since this discovery, there have been considerable efforts to optimize the storage capacities in hydrates through the variability of the formation condition, of the cage occupancy, of the chemical composition or of the hydrate structure (ranging from clathrate to semi-clathrate). In addition to this issue, the hydrogen insertion mechanism plays also a crucial role not only at a fundamental level, but also in view of potential applications. This paper aims at studying the molecular hydrogen diffusion in the THF hydrate by *in-situ* confocal Raman microspectroscopy and imaging, and at investigating the impact of strong acid onto this diffusive process. This study represents the first report to shed light on hydrogen diffusion in acidic THF-H₂ hydrate. Integrating the present result with those from previous experimental investigations, it is shown that the hydrogen insertion in the THF hydrate is optimum for a pressure of ca. 55 bar at 270 K. Moreover, the co-inclusion of perchloric acid (with concentration as low as 1 acidic molecules per 136 water molecules) lead to promote the molecular hydrogen insertion within the hydrate structure. The hydrogen diffusion coefficient—measured at 270 K and 200 bar—is improved by a factor of 2 thanks to the acidic additive.

Keywords: strong acid, hydrogen storage, tetrahydrofuran, hydrates, clathrates, Raman spectroscopy

OPEN ACCESS

Edited by:

Amadeu K. Sum,
Colorado School of Mines,
United States

Reviewed by:

Kyuchul Shin,
Kyungpook National University,
South Korea
Ryo Ohmura,
Keio University, Japan

*Correspondence:

Arnaud Desmedt
arnaud.desmedt@u-bordeaux.fr

Specialty section:

This article was submitted to
Physical Chemistry and Chemical
Physics,
a section of the journal
Frontiers in Chemistry

Received: 10 April 2020

Accepted: 03 September 2020

Published: 14 October 2020

Citation:

Nguyen TT, Pétuya C, Talaga D and
Desmedt A (2020) Promoting the
Insertion of Molecular Hydrogen in
Tetrahydrofuran Hydrate With the Help
of Acidic Additives.
Front. Chem. 8:550862.
doi: 10.3389/fchem.2020.550862

INTRODUCTION

Hydrogen is the most abundant element on Earth and is considered as a clean and potential energy vector in the future. H₂ storage and transportation are the subject of numerous studies. Among gas storage materials, hydrogen clathrate hydrates (also called hydrates) have received a particular attention over the last decades (Florusse et al., 2004; Veluswamy et al., 2014). Gas hydrates are crystalline inclusion compounds of hydrogen bonded water molecules forming cages encapsulating guest molecules (Sloan and Koh, 2008; Broseta et al., 2017; Ruffine et al., 2018). The pure H₂ clathrate hydrate is generated only at extremely high-pressure (few thousands of bars) and at low temperature (~240 K) (Dyadin et al., 1999; Mao et al., 2002). The hydrate is then formed with H₂ molecular species located in the small cages (SC) and in the large cages (LC) of the so-called sII hydrate (consisting of 16 SCs and 8 LCs) (Mao et al., 2002). To enable the storage of H₂ under softer conditions (typically 50 bars and 280 K), the method consists in co-including H₂ molecules

with a second guest such as tetrahydrofuran (THF), to form a mixed THF-H₂ sII hydrate (Florusse et al., 2004; Lee et al., 2005). However, THF molecules occupy the LC and H₂ molecules are only in the SC, which leads to low hydrogen storage (<2 wt%) (Strobel et al., 2006; Mulder et al., 2008) and limits the potential applications (Nakayama et al., 2010). Since this discovery, there have been considerable efforts to optimize the storage capacities of H₂ in clathrate hydrates through the variability of the formation condition, of the cage occupancy, of the chemical composition (by changing the promoter and its concentration) or of the cage structure (from clathrate to semi-clathrate) (Veluswamy et al., 2014).

Beyond the problematic of H₂ storage capacity for potential applications, the H₂ insertion mechanism plays is of fundamental interest. When H₂ gas pressure is applied onto a powdered THF hydrate, the formation mechanism involves two steps: hydrogen adsorption onto the clathrate particle surface, followed by subsequent diffusion of hydrogen into the clathrate hydrate particle. The inter-cage diffusion represents the limiting step (timescale of the order of days), involving high activation energy (78.7 kJ/mol) (Nagai et al., 2008), confirmed by electronic structure calculations (Alavi and Ripmeester, 2007). To improve the storage capability of H₂ in hydrates, one issue concerns the possibility of modifying the water cage relaxation. The dynamic properties of various hydrates have been investigated and water molecules reorients on a millisecond timescale (Sloan and Koh, 2008). Recently, it has been shown that water molecules relax on a nanosecond timescale in strong acid clathrate hydrates (Desmedt et al., 2004, 2013; Bedouret et al., 2014). Moreover, THF clathrate hydrate may be prepared by co-including strong acid molecules (Desmedt et al., 2015). Such chemical modification has an impact onto the lattice dynamics of the cages and on the melting points of the hydrates (Desmedt et al., 2015). However, to the best of our knowledge, no studies have been performed until now to investigate the H₂ storage in such THF clathrate hydrates co-including strong acid species.

The description of the H₂ insertion mechanism outlines the key role played by dynamical processes met in clathrate hydrates (Desmedt et al., 2012, 2017). At atmospheric pressure, only intra-cage diffusion of H₂ is experimentally observed in the THF-H₂ hydrate stability region (i.e., below *ca.* 270 K) (Pefoute et al., 2012). At higher pressure (typically several tens of bars), studies of molecular hydrogen diffusion into THF hydrates have been performed by means of NMR method (Okuchi et al., 2007), *in situ* neutron diffraction (Mulder et al., 2008), volumetric measurements (Nagai et al., 2008), theoretical calculations (Alavi and Ripmeester, 2007) and molecular dynamics simulations (Cao et al., 2013). These measurements, performed in various P-T thermodynamics conditions, lead to diffusion coefficient ranging from *ca.* 10⁻⁶ cm²/s to *ca.* 10⁻¹² cm²/s. These results outline the importance of using an experimental method allowing the direct investigation of the spatial and time characteristics of the H₂ diffusion within the hydrate. In this issue, confocal Raman microspectroscopy is a non-destructive approach and is particularly adapted for *in situ* investigation of transport process in nanoporous systems (Marti-Rujas et al., 2004, 2006, 2007). This vibrational technique is an interesting label-free tool to

access the molecular composition, the molecular selectivity, the structural and dynamical information in gas hydrates (Chazallon et al., 2017; Petuya et al., 2017, 2018a,b; Petuya and Desmedt, 2019). Raman spectroscopy has been performed to study the hydrogen storage in hydrates (Florusse et al., 2004; Ogata et al., 2008; Strobel et al., 2009; Grim et al., 2012) and it has been shown that THF hydrates may act as a molecular sieving for hydrogen-containing gas mixtures (Zhong et al., 2017). This paper aims at studying the H₂ diffusion mechanism in the THF clathrate hydrate by *in situ* confocal Raman microspectroscopy and imaging, and at investigating the impact of strong acid onto this diffusive process at 200 bar pressure. To address this issue, we use two different sII hydrogen hydrate formed with THF promoter: THF-H₂ hydrate (non-acidic) and the THF-HClO₄-H₂ hydrate (acidic).

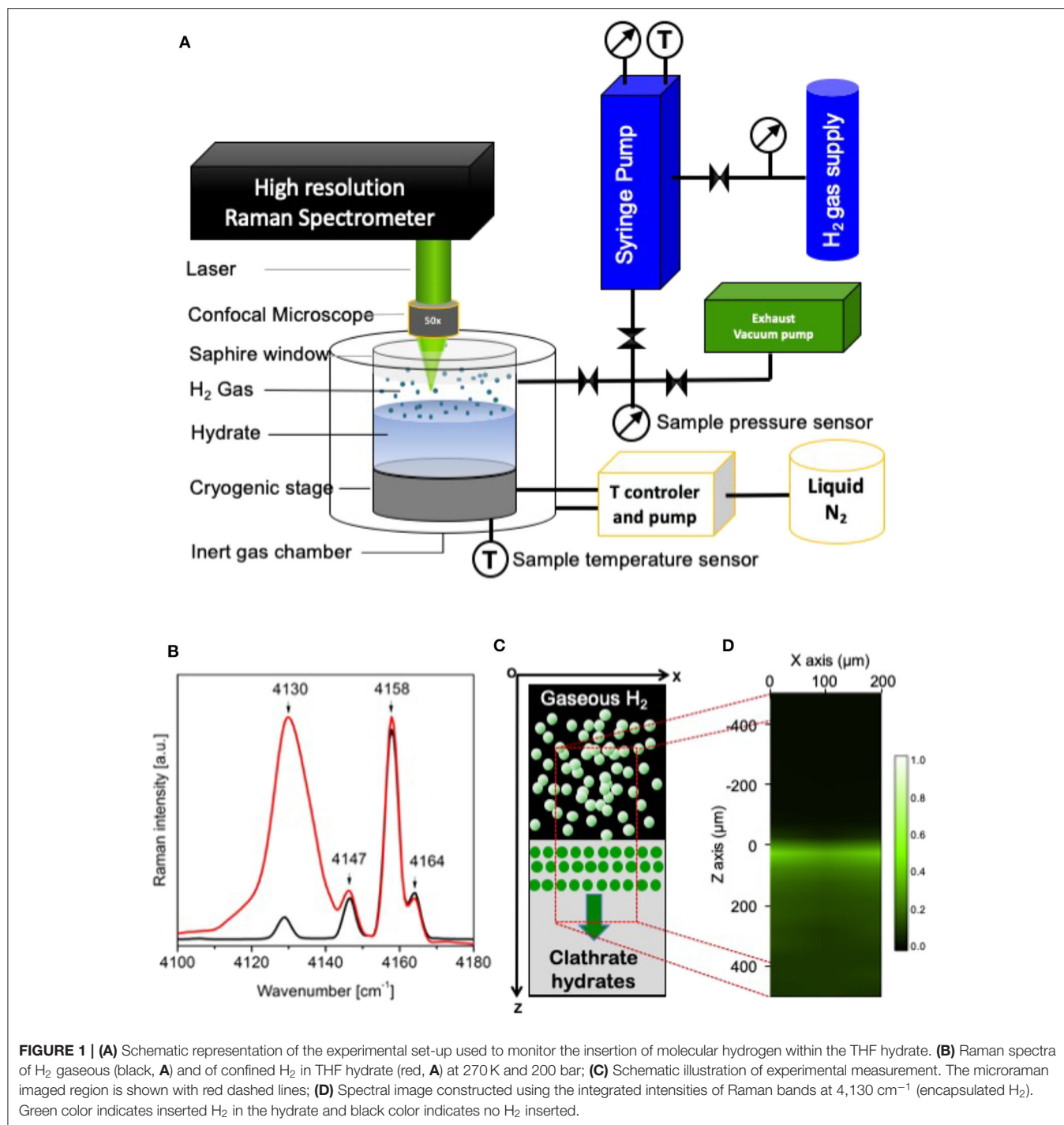
EXPERIMENTAL DETAILS

Samples

Two solutions were prepared with the following molar ratio 8THF·136H₂O (melting at 277 K) and 7THF⁻1HClO₄·136H₂O (melting at 271 K) using ultra-pure water (Milli-Q quality) and commercially available chemicals (70% HClO₄ aqueous solution and 99.9% THF from Sigma-Aldrich). They were transferred under inert atmosphere in the lab-made high-pressure optical cell used for the Raman spectroscopic analysis. According to a procedure previously published (Desmedt et al., 2015), the hydrates have been formed under stirring conditions by cooling the sample temperature to 270 K and maintaining this temperature for 24 h with the help of a modified cryogenic stage (Linkam Scientific Instruments Ltd., UK). Once the hydrate is formed, hydrogen gas (99.9999% Air Liquide) was then applied at constant pressure (200 bar) with a PM High Pressure pump (Top Industrie, Vaux-le-Penil, France) which contains 100 cm³ of gas.

Raman Scattering and Imaging

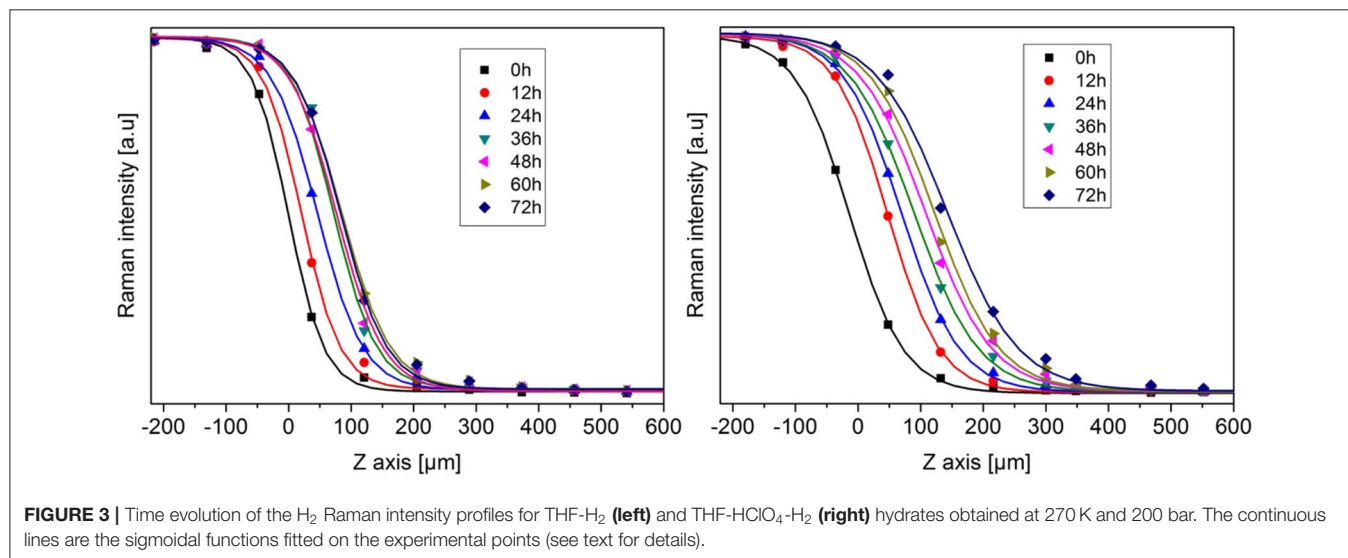
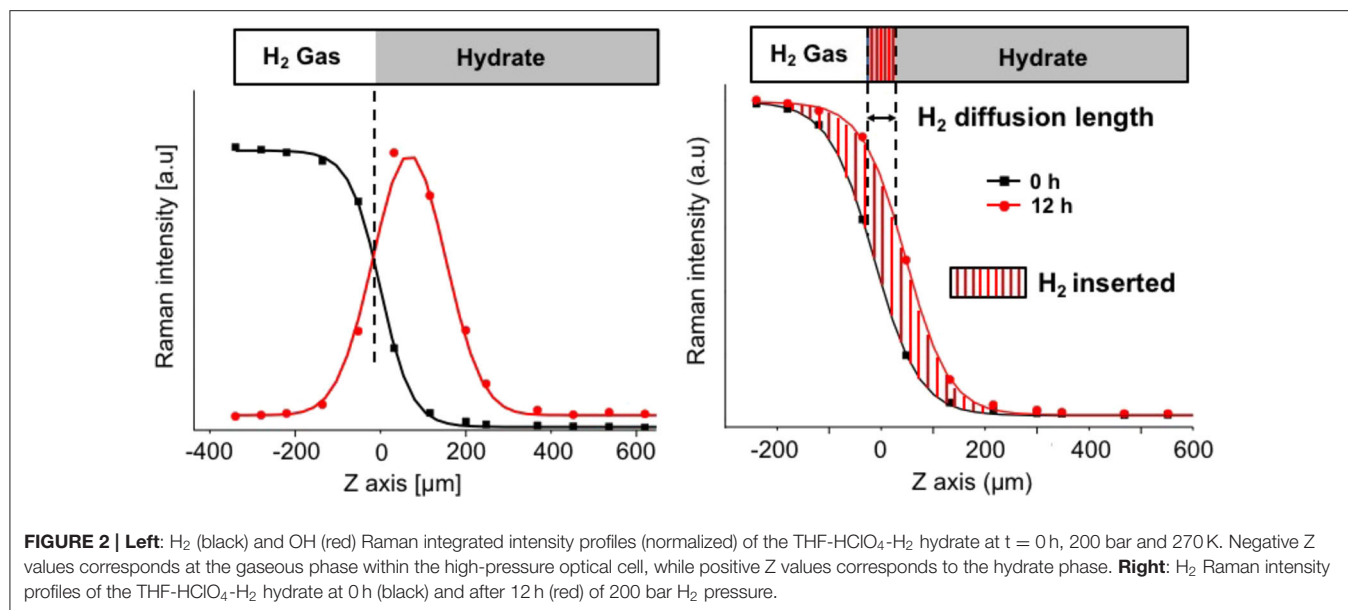
Raman data were collected with a Labram microspectrometer (Horiba Jobin Yvon, Villeneuve d'Ascq, France) and using a 514 nm laser source (10 mW power at the sample). A 50X objective (NA = 0.45, Olympus) permitted to focus the incident laser beam and to collect the Raman scattering. The Raman scattering was dispersed with a holographic grating of 1,800 g/mm and analyzed with a Peltier-cooled CCD detector (Andor, Belfast, UK), which permitted to measure the Raman spectra with a spectral resolution of 1 cm⁻¹. The data was collected on a spectral range from 2,700 to 4,300 cm⁻¹ to monitor the hydrogen stretching modes. To probe the H₂ diffusion into the preformed hydrate as a function of time, micro-Raman spectra and imaging were collected *in situ* under the 200 bar H₂ pressure at 270 K in the hydrate stability zone (Hashimoto et al., 2007). The measurement has been started simultaneously with the application of H₂ pressure (corresponding to time *t* = 0 h in the following). For recording the spectral images, a motorized stage was used to map the sample in a point-by-point mode using a 20 μm step size in the two XZ plane perpendicular to the gas-hydrate interface contained in the XY plane (**Figure 1**). For each



sample, an area of about $200 \times 1,200 \mu\text{m}^2$ from the H₂/hydrate interface to 1,000 μm depths in the hydrate by Raman micro-imaging. In the following, $Z = 0 \mu\text{m}$ corresponds to the gas-hydrate interface. Raman intensity depth profiles of inserted H₂ were corrected from the refraction by using standard procedure (Everall, 2000; Desmedt et al., 2007) with a refraction index $n = 1,33$ (Sloan and Koh, 2008) for the hydrate.

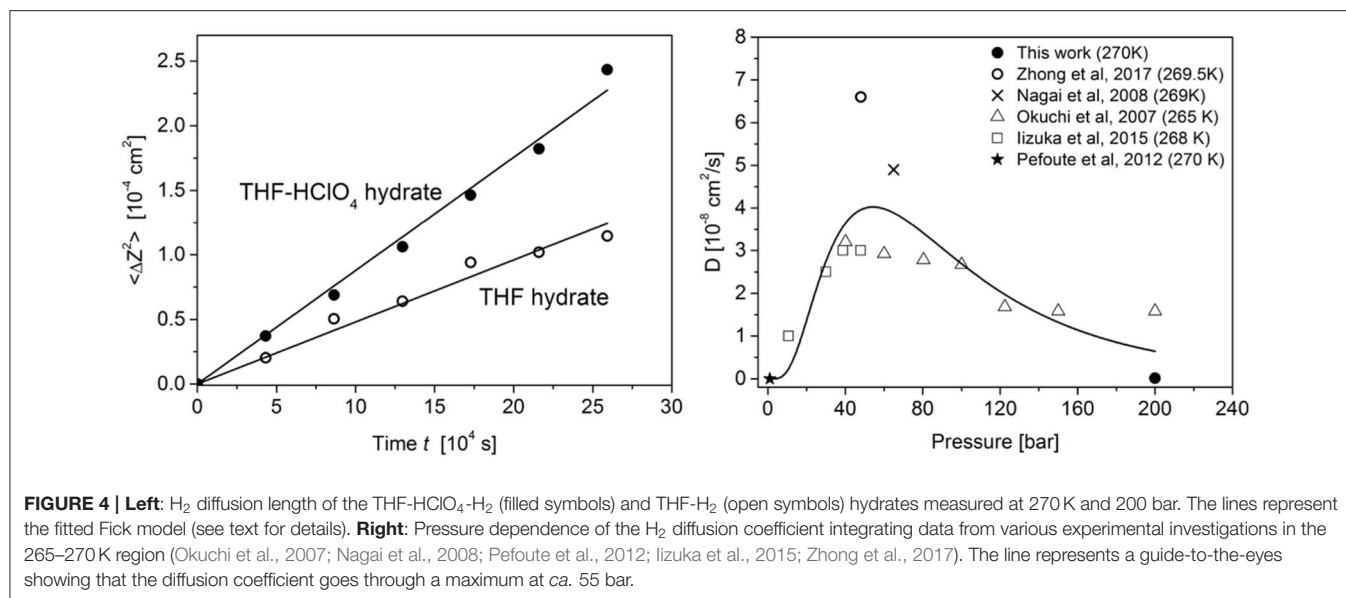
RESULTS AND DISCUSSION

In the present investigation, two hydrates have been considered: the THF hydrate (formed with a THF·17H₂O solution) and the mixed THF-HClO₄ hydrate (formed with a 0.875THF·0.125HClO₄·17H₂O solution). In these sII hydrates, the SCs are empty to welcome H₂ molecules, the THF molecules occupy the



LC and the acidic additive HClO₄ is inserted within the LC by replacing one THF per unit cell in average (Desmedt et al., 2015). The insertion of molecular hydrogen within these two preformed hydrates has been probed thanks to real-time Raman imaging. An example of the spectral region corresponding to the gaseous H₂ and confined H₂ signatures is shown in **Figure 1A** for the THF-H₂ hydrate formed within the lab-made high-pressure optical cell after 1 day at 200 bars and 270 K. The rotation-vibration coupled bands of gaseous H₂ are observed at 4,130, 4,147, 4,155, and 4,164 cm⁻¹. In the case of the THF-H₂ hydrate, the band at 4,130 cm⁻¹ is assigned to the Raman signal of H₂ confined in the sII hydrate SCs (Ogata et al., 2008; Strobel et al., 2009; Grim et al., 2012). To monitor the insertion of hydrogen within the hydrate, Raman imaging has been performed in the plane

perpendicular to the gas/hydrate interface (see **Figure 1B**). An example of visualization of the H₂ molecules confined in the hydrate is shown in **Figure 1C** through the Raman mapping of the ratio of the band intensity at 4,130 cm⁻¹ and of the one at 4,155 cm⁻¹. The Raman intensity being proportional to the encapsulated species concentration (Zhong et al., 2017), such a Raman image is a direct signature of the spatial H₂ distribution within the preformed THF hydrate; after 1 day of pressurization, one can observe that H₂ has mainly been inserted within few tens of micrometers below the hydrate surface. In order to spatially analyse the extension of H₂ insertion, one needs to locate the gas/hydrate interface at a micrometric scale. In this purpose, the intensity profiles of the H₂ vibron and of the OH stretching modes have been measured with the help of



the projection of the acquired Raman spectra in the XZ plane along the Z axis (see **Figure 1B**). An example of such averaged profiles is shown in **Figure 2** (left) for the measurement at initial stage ($t = 0$ h) of H₂ pressurization at 200 bar and at $T = 270$ K. A pseudo-Voigt function has been used to reproduce the experimental data of the OH integrated intensity profile and the H₂ intensity profile has been fitted with a sigmoidal function. The fitted functions reproduce with a good agreement the experimental data (the residual error between experimental and modeled curves reached a value of 10^{-3}). The gas/hydrate interface is then clearly identified at the intersection of these two curves: it corresponds to the Z coordinate of the inflection point of the H₂ sigmoidal curve. This procedure allows to accurately determine the Z position of the gas/hydrate interface and is set as the reference distance $Z = 0 \mu\text{m}$. Moreover, the H₂ vibron intensity profile can be used as a signature of the H₂ diffusion front position as a function of time. This is shown in **Figure 2** (right): the H₂ intensity profiles of THF-HClO₄-H₂ hydrate after 12 h of pressurization is clearly Z-shifted with respect to the profile at initial time $t = 0$ h. This Z difference of the H₂ diffusion front is the signature of the insertion of H₂ molecule within the hydrate sample; it is defined as the mean H₂ diffusion length, $\Delta Z(t)$:

$$\langle \Delta Z(t) \rangle = Z(t) - Z(0) \quad (1)$$

where $Z(t)$ corresponds to the inflection point of the H₂ sigmoidal curve at time t . To subsequently analyse the time-evolution of the H₂ insertion, such H₂ Raman intensity profiles have been recorded every 12 h over a period of 3 days. In order to evaluate the impact of the strong acid HClO₄ additive, these measurements have been performed onto the preformed THF hydrate and onto the preformed THF-HClO₄ hydrate, both pressurized with H₂ gas at 270 K and 200 bar. The time evolution of the H₂ intensity profiles is shown in **Figure 3** for the

THF-HClO₄-H₂ hydrate and for the THF-H₂ hydrate. It can be observed a marked difference between these time evolutions: the H₂ diffusion front extend over a wider range in the case of the THF-HClO₄ hydrates compared to the case of the THF hydrate, i.e., without acidic additives. In order to quantitatively analyse the time evolution of the H₂ diffusion front within the hydrates, each intensity profile has been fitted by using the sigmoidal function as previously described, allowing to measure the position of the H₂ diffusion front as a function of time. Such procedure allows to measure the H₂ diffusion lengths (Equation 1) as a function of time. Their mean-squared values $\langle \Delta Z(t)^2 \rangle$ are reported in **Figure 4**. These curves show clearly the improvement of the H₂ insertion when acidic additives are included in the THF hydrate: the values are higher for the THF-HClO₄ hydrate than for the THF hydrate.

Furthermore, such curves provide the opportunity to investigate the H₂ insertion mechanism. Such diffusive mechanism may include various elementary processes including the inter-cage diffusion and possible contributions associated with grain boundaries, chemical and structural defects. Let first consider two principal diffusive models by analogy with nanoporous systems (Marti-Rujas et al., 2007): conventional diffusion or single-file-like diffusion. The conventional diffusion corresponds to the Fick law for which the mean-squared H₂ diffusion length is given by the Einstein diffusion model in a three-dimensional system:

$$\langle \Delta Z(t)^2 \rangle = 6Dt \quad (2)$$

where D is the H₂ diffusion coefficient. The Fick behavior may reproduce not only the inter-cage diffusion, but also the diffusion associated with grain boundaries and structural defects. The single-file-like diffusive model may be considered for the H₂ inter-cage diffusion. Indeed, the H₂ molecule dimension is

comparable to the diameter of the polygonal faces of the water cages. In such a model, H₂ molecule diffusion within a water cage may proceed under the condition that there is a vacant guest site in the neighboring cage—unlike in the case of Fick behavior for which H₂ molecules can overtake each other in the cages. This phenomenon involves correlations between the H₂ displacements within the hydrate and thus the time-dependence of $\langle \Delta Z(t)^2 \rangle$ differs from the Fick diffusion:

$$\langle \Delta Z(t)^2 \rangle = 6Mt^{1/2} \quad (3)$$

where M correspond to the H₂ mobility in the three-dimensional hydrate system. The time dependence of $\langle \Delta Z(t)^2 \rangle$ exhibit a clear linear behavior (it has not been possible to reproduce the experimental data with the single-file-like model). It thus implies that H₂ molecules can overtake each other in a cage and mainly follows a fick behavior. such a diffusive behavior is in full agreement with NMR (Okuchi et al., 2007), *in situ* neutron diffraction (Mulder et al., 2008), volumetric measurements (Nagai et al., 2008), Raman (Zhong et al., 2017), and molecular dynamics (Cao et al., 2013). The Fick law given by Equation (2) have been fitted to the experimental data with an excellent agreement (see **Figure 4-Left**). The fitted diffusion coefficients are of $7.98 \pm 0.03 \cdot 10^{-11}$ cm²/s for the THF hydrate and $1.46 \pm 0.03 \cdot 10^{-10}$ cm²/s for the THF-HClO₄ hydrate at 270 K and 200 bar. The obtained diffusion coefficient for the H₂ insertion in the THF-H₂ hydrate is within the broad range of values obtained by various experimental methods and reported in **Figure 4-Right**. The present study confirms the trend of an optimum pressure for promoting the hydrogen diffusion at *ca.* 55 bar. Such a behavior reflects a trend regarding the transport of hydrogen molecules between the cages: the inter-cage diffusion is slower when a large fraction of the small cage is already filled, or even doubly filled with H₂ as reported from Molecular Dynamics simulations (Cao et al., 2013). Once the small cage of the sII THF hydrate are filled, structural or chemical defects and grain boundaries should play a key-role for insuring the Fickian H₂ diffusion through and within the sII THF hydrate. Indeed, the behavior observed with the THF-HClO₄ hydrate confirms the importance of such defects: a clear quantitative enhancement of the H₂ diffusion in the THF hydrate is measured thanks to the co-inclusion of HClO₄ in the sII structure (**Figure 4-Left**). As reported in previous studies (Desmedt et al., 2015), the inclusion of HClO₄ into the THF hydrate lead to generate perchlorate anions confined in the LC and acidic protons delocalized within the water cage structure (this delocalization is at the origin of the super-protonic conductivity met in strong acid hydrates; Desmedt et al., 2004, 2013). In such a case, the cages are constituted not only of water molecules, but also of hydronium ions. The energy barrier related to H₂ molecules diffusion through the water cage being higher for SC than for LC (Okuchi et al., 2007), the inclusion of such ionic defects in the hydrate lead to modify the flexibility of the cage, as reported from Raman measurements of the water cage phonons (Desmedt et al., 2015). This increased flexibility of the

water cage—especially of the SCs welcoming the H₂—may lead to decrease the energy barrier required for an H₂ molecule to cross the faces of the water cage and thus to facilitate the inter-cage diffusion, as reflected by the enhanced diffusion coefficient measured in the THF-HClO₄.

CONCLUSION

The present investigation represents the first report to shed light on the impact of ionic defects onto the hydrogen insertion within hydrate. This study has been realized by comparing the H₂ diffusion within the THF hydrate and the mixed THF-HClO₄ hydrate, both being sII structure. Raman confocal microspectroscopy and imaging has been a powerful tool. It yields the measurement of the H₂ Fickian diffusion coefficients within the two hydrates at 270 K and 200 bar: $7.98 \pm 0.03 \cdot 10^{-11}$ cm²/s for the THF hydrate and $1.46 \pm 0.03 \cdot 10^{-10}$ cm²/s for the THF-HClO₄ hydrate. In the case of the THF hydrate, it is shown that the H₂ diffusion within the hydrate is optimum for a pressure of *ca.* 55 bar by compiling this result with those from the literature. Moreover, this investigation clearly shows the enhancement of the H₂ insertion within the THF hydrate thanks to the co-inclusion of acidic additive: it acts as a “flexibilizer” of the water cage through the addition of chemical water H-bond defects (Desmedt et al., 2015) promoting the H₂ inter-cage diffusion. Such results are particularly exciting and promising for applications in storage of hydrogen and open new routes for developing efficient hydrate-based hydrogen storage materials with new type of promoter.

DATA AVAILABILITY STATEMENT

The original contributions presented in the study are included in the article/supplementary material, further inquiries can be directed to the corresponding author/s.

AUTHOR CONTRIBUTIONS

TN and CP have performed the sample preparation, the Raman scattering experiments, and data acquisition. DT has contributed to the Raman spectrometer configuration and data management. TN and AD has analyzed, interpreted the data, and has written the manuscript. All authors contributed to the article and approved the submitted version.

FUNDING

This work falls in the frame of the project ANR 2011-JS08-002-01, funded by the French ANR Agence Nationale de la Recherche. The Raman scattering experiments have been performed on equipment of the Vibrational Spectroscopy and Imaging platform (SIV at ISM), funded by the Conseil Régional de Nouvelle Aquitaine and Europe (FEDER programme).

REFERENCES

- Alavi, S., and Ripmeester, J. A. (2007). Hydrogen-gas migration through clathrate hydrate cages. *Angew. Chem. Int. Ed.* 46, 6102–6105. doi: 10.1002/ange.200790242
- Bedouret, L., Judeinstein, P., Ollivier, J., Combet, J., and Desmedt, A. (2014). Proton diffusion in the hexafluorophosphoric acid clathrate hydrate. *J. Phys. Chem. B* 118, 13357–13364. doi: 10.1021/jp504128m
- Broseta, D., Ruffine, L., and Desmedt, A. (2017). *Gas Hydrates 1: Fundamentals, Characterization and Modeling*. London: Wiley–ISTE.
- Cao, H., English, N. J., and MacElroy, J. M. D. (2013). Diffusive hydrogen inter-cage migration in hydrogen and hydrogen-tetrahydrofuran clathrate hydrates. *J. Chem. Phys.* 138:094507. doi: 10.1063/1.4793468
- Chazallon, B., Noble, J., and Desmedt, A. (2017). “Spectroscopy of gas hydrates: from fundamental aspects to chemical engineering, geophysical and astrophysics applications,” in *Gas Hydrates 1: Fundamentals, Characterization and Modeling*, eds D. Broseta, L. Ruffine, and A. Desmedt (London, UK: Wiley–ISTE), 63–112.
- Desmedt, A., Bedouret, L., Ollivier, J., and Petuya, C. (2017). “Neutron scattering of clathrate and semi-clathrate hydrates,” in *Gas Hydrates 1: Fundamentals, Characterization and Modeling*, eds D. Broseta, L. Ruffine, and A. Desmedt (London, UK: Wiley–ISTE), 1–62. doi: 10.1002/9781119332688.ch1
- Desmedt, A., Bedouret, L., Pefoute, E., Pouvreau, M., Say-Liang-Fat, S., and Alvarez, M. (2012). Energy landscape of clathrate hydrates. *Eur. Phys. J. Special Topics* 213, 103–127. doi: 10.1140/epjst/e2012-01666-3
- Desmedt, A., Lechner, R. E., Lassègues, J. C., Guillaume, F., Cavagnat, D., and Grondin, J. (2013). Hydronium dynamics in the perchloric acid clathrate hydrate. *Solid State Ion.* 252, 19–25. doi: 10.1016/j.ssi.2013.06.004
- Desmedt, A., Martin-Gondre, L., Nguyen, T. T., Petuya, C., Barandiaran, L., Babot, O., et al. (2015). Modifying the flexibility of water cages by co-including acidic species within clathrate hydrate. *J. Phys. Chem. C* 119, 8904–8911. doi: 10.1021/jp511826b
- Desmedt, A., Stallmach, F., Lechner, R. E., Cavagnat, D., Lassègues, J. C., Guillaume, F., et al. (2004). Proton dynamics in the perchloric acid clathrate hydrate $\text{HClO}_4\cdot 5.5\text{H}_2\text{O}$. *J. Chem. Phys.* 121, 11916–11926. doi: 10.1063/1.1819863
- Desmedt, A., Talaga, D., and Bruneel, J. L. (2007). Enhancement of the raman scattering signal due to a nanolens effect. *Appl. Spectroscop.* 61, 621–623. doi: 10.1366/000370207781269837
- Dyadin, Y. A., Larionov, E. G., Aladko, E. Y., Manakov, A. Y., Zhurko, F. V., Mikina, T. V., et al. (1999). Clathrate formation in water-noble gas (Hydrogen) systems at high pressures. *J. Struct. Chem.* 40, 790–795. doi: 10.1007/BF02903454
- Everall, N. J. (2000). Modeling and measuring the effect of refraction on the depth resolution of confocal raman microscopy. *Appl. Spectrosc.* 54:773. doi: 10.1366/0003702001950382
- Florusse, L. J., Peters, C. J., Schoonman, J., Hester, K. C., Koh, C., Dec, S. F., et al. (2004). Stable low-pressure hydrogen clusters stored in a binary clathrate hydrate. *Science* 306:469–471. doi: 10.1126/science.1102076
- Grim, R. G., Kerkar, P. B., Shebowich, M., Arias, M., Sloan, E. D., Koh, C. A., et al. (2012). synthesis and characterization of sI clathrate hydrates containing hydrogen. *J. Phys. Chem. C* 116, 18557–18563. doi: 10.1021/jp307409s
- Hashimoto, S., Sugahara, T., Sato, H., and Ohgaki, K. (2007). Thermodynamic stability of H_2 + tetrahydrofuran mixed gas hydrate in nonstoichiometric aqueous solutions. *J. Chem. Eng. Data* 52, 517–520. doi: 10.1021/je060436f
- Iizuka, A., Hayashi, S., Tajima, H., Kiyono, F., Yanagisawa, Y., and Yamasaki, A. (2015). Gas separation using tetrahydrofuran clathrate hydrate crystals based on the molecular sieving effect. *Sep. Purif. Technol.* 139, 70–77. doi: 10.1016/j.seppur.2014.10.023
- Lee, H., Lee, J., Kim, D. Y., Park, J., Seo, Y.-T., Zeng, H., et al. (2005). Tuning clathrate hydrates for hydrogen storage. *Nature* 434, 743–746. doi: 10.1038/nature03457
- Mao, W. L., Mao, H. K., Goncharov, A. F., Struzhkin, V. V., Guo, Q. Z., Hu, J. Z., et al. (2002). Hydrogen clusters in clathrate hydrate. *Science* 297, 2247–2249. doi: 10.1126/science.1075394
- Marti-Rujas, J., Desmedt, A., Harris, K. D. M., and Guillaume, F. (2004). Direct time-resolved and spatially resolved monitoring of molecular transport in a crystalline nanochannel system. *J. Am. Chem. Soc.* 126, 11124–11125. doi: 10.1021/ja040117d
- Marti-Rujas, J., Desmedt, A., Harris, K. D. M., and Guillaume, F. (2007). Kinetics of molecular transport in a nanoporous crystal studied by confocal raman microspectrometry: single-file diffusion in a densely filled tunnel. *J. Phys. Chem. B. (Letter)* 111, 12339–12344. doi: 10.1021/jp076532k
- Marti-Rujas, J., Harris, K. D. M., Desmedt, A., and Guillaume, F. (2006). Significant conformational changes associated with molecular transport in a crystalline solid. *J. Phys. Chem. B* 110, 10708–10713. doi: 10.1021/jp060738o
- Mulder, F. M., Wagemaker, M., van Eijck, L., and Kearley, G. J. (2008). Hydrogen in porous tetrahydrofuran clathrate hydrate. *Chem. Phys. Chem.* 9, 1331–1337. doi: 10.1002/cphc.200700833
- Nagai, Y., Yoshioka, H., Ota, M., Sato, Y., Inomata, H., Smith, J. R., et al. (2008). Binary hydrogen-tetrahydrofuran clathrate hydrate formation kinetics and models. *AiChE J.* 54, 3007–3016. doi: 10.1002/aic.11587
- Nakayama, T., Tomura, S., Ozaki, M., and Mori, H. M. (2010). Engineering investigation of hydrogen storage in the form of clathrate hydrates: conceptual design of hydrate production plants. *Energy Fuels* 24, 2576–2588. doi: 10.1021/ef100039a
- Ogata, K., Hashimoto, S., Sugahara, T., Moritoki, M., Sato, H., and Ohgaki, K. (2008). Storage capacity of hydrogen in tetrahydrofuran hydrate. *Chem. Eng. Sci.* 63, 5714–5718. doi: 10.1016/j.ces.2008.08.018
- Okuchi, T., Moudrakovski, I. L., and Ripmeester, J. A. (2007). Efficient storage of hydrogen fuel into leaky cages of clathrate hydrate. *Appl. Phys. Lett.* 91:171903. doi: 10.1063/1.2802041
- Pefoute, E., Kemner, E., Soetens, J. C., Russina, M., and Desmedt, A. (2012). Diffusive motions of molecular hydrogen confined in THF clathrate hydrate. *J. Phys. Chem. C* 116, 16823–16829. doi: 10.1021/jp3008656
- Petuya, C., Damay, F., Chazallon, B., Bruneel, J. L., and Desmedt, A. (2018a). Guest partitioning and metastability of the nitrogen gas hydrate. *J. Phys. Chem. C* 122, 566–573. doi: 10.1021/acs.jpcc.7b10151
- Petuya, C., Damay, F., Desplanche, S., Talaga, D., and Desmedt, A. (2018b). Selective trapping of CO_2 gas and cage occupancy in $\text{CO}_2\text{-N}_2$ and $\text{CO}_2\text{-CO}$ mixed gas hydrates. *Chem. Comm.* 54, 4290–4293. doi: 10.1039/C8CC00538A
- Petuya, C., Damay, F., Talaga, D., and Desmedt, A. (2017). Guest partitioning in carbon monoxide hydrate by raman spectroscopy. *J. Phys. Chem. C* 121, 13798–13802. doi: 10.1021/acs.jpcc.7b04947
- Petuya, C., and Desmedt, A. (2019). Revealing CO-preferential encapsulation in the mixed CO-N_2 clathrate hydrate. *J. Phys. Chem. C* 123, 4871–4878. doi: 10.1021/acs.jpcc.8b11680
- Ruffine, L., Broseta, D., and Desmedt, A. (2018). *Gas Hydrates 2: Geoscience Issues and Potential Industrial Applications*. London: Wiley–ISTE.
- Sloan, E. D., and Koh, C. A. (2008). *Clathrate Hydrates of Natural Gases*. Boca Raton, FL: CRC Press.
- Strobel, T. A., Sloan, E. D., and Koh, C. A. (2009). Raman spectroscopic studies of hydrogen clathrate hydrates. *J. Chem. Phys.* 130:014506. doi: 10.1063/1.3046678
- Strobel, T. A., Taylor, C. J., Hester, K. C., Dec, S. F., Koh, C. A., Miller, K. T., et al. (2006). Molecular hydrogen occupancy in binary THF– H_2 clathrate hydrates by high resolution neutron diffraction. *J. Phys. Chem. B* 110, 14024–14027. doi: 10.1021/jp062139n
- Veluswamy, H. P., Kumar, R., and Linga, P. (2014). Hydrogen storage in clathrate hydrates: current state of the art and future directions. *Appl. Energy* 122, 112–132. doi: 10.1016/j.apenergy.2014.01.063
- Zhong, J. R., Chen, L. T., Liu, T. C., Zeng, X. Y., Sun, Y. F., Sun, C. Y., et al. (2017). Sieving of hydrogen-containing gas mixtures with tetrahydrofuran hydrate. *J. Phys. Chem. C* 121, 27822–27829. doi: 10.1021/acs.jpcc.7b08945

Conflict of Interest: The authors declare that the research was conducted in the absence of any commercial or financial relationships that could be construed as a potential conflict of interest.

Copyright © 2020 Nguyen, Pétuya, Talaga and Desmedt. This is an open-access article distributed under the terms of the Creative Commons Attribution License (CC BY). The use, distribution or reproduction in other forums is permitted, provided the original author(s) and the copyright owner(s) are credited and that the original publication in this journal is cited, in accordance with accepted academic practice. No use, distribution or reproduction is permitted which does not comply with these terms.